

Influence of the Galactic gravitational field on the positional accuracy of extragalactic sources.
II Observational appearances and detectability

TATIANA I. LARCHENKOVA,¹ NATALIA S. LYSKOVA,^{2,3,1} LEONID PETROV,⁴ AND ALEXANDER A. LUTOVINOV^{3,2}

¹*P.N.Lebedev Physical Institute, Leninskiy prospect 53, Moscow 119991, Russia*

²*National Research University Higher School of Economics, Myasnitskaya str. 20, Moscow 101000, Russia*

³*Space Research Institute (IKI), Russian Academy of Sciences, Profsoyuznaya 84/32, 117997 Moscow, Russia*

⁴*NASA GSFC, 8800 Greenbelt Rd, Greenbelt, MD 20771 USA*

(Received xxx, 2020; Revised yyy; Accepted zzz)

ABSTRACT

We consider a possibility of detecting the jitter effect of apparent celestial positions of distant sources due to local fluctuations of the Galaxy gravitational field. It is proposed to observe two samples of extragalactic sources (target and control) in different sky directions using the high-precision radio interferometry. It is shown that on a scale of ~ 2 years, it is possible to detect a systematic increase in the standard deviation of measured arc lengths of pairs of target sources compared to the control ones at the 3σ -level if the accuracy of differential astrometric observations is around $10 \mu\text{as}$. For the current state-of-the-art accuracy of $30 \mu\text{as}$ achieved at the KVN or VERA interferometers, which have shorter baselines in comparison with VLBI, the target and control samples will differ only at the 2σ -level on the scale of 10 years. To achieve the 3σ -level on this time interval, it is necessary to improve the accuracy up to $\sim 20 \mu\text{as}$. Other possible effects that can also affect the arc length measurements between two sources are discussed, and an observational strategy to minimize them is suggested.

Keywords: Galaxy: general - gravitation - astrometry

1. INTRODUCTION

Before reaching an observer, an electromagnetic radiation of extragalactic sources propagates through the gravitational field of our Galaxy. While stationary on large scales, the gravitational field of the Galaxy is subject to local fluctuations due to motions of stars, compact relativistic objects and invisible compact halo objects. These inhomogeneities could lead to different observational appearances, in particular, to variations with time in an apparent position of any extragalactic sources (a so-called “jitter”). In particular, active galactic nuclei (AGNs) have ultra-compact cores associated with supermassive black holes (SMBHs). Nowadays, positions of such cores can be determined with sub-nanoradian accuracies using a very long baseline interferometry (VLBI, Beasley et al. 2002) or space astrometry, e.g. *Gaia* (Lindgren et al. 2018). A transversal motion of SMBHs located at cosmological distances is supposed to be very small, well below $1 \mu\text{as}/\text{year}$. The gravitational deflection in the inhomogeneous non-stationary gravitational field of the Galaxy will cause the

jitter in apparent positions of an AGN core. This effect imposes a fundamental constraint on the achievable accuracy of high-precision astrometric observations. Due to the high importance, this topic has been actively investigated since the nineties of the last century (see, e.g. Zhdanov & Zhdanova 1995; Dominik & Sahu 2000; Yano 2012; Larchenkova et al. 2017, and references therein).

In the recent paper of Larchenkova et al. (2017) (hereafter Paper I), an influence of random variations of the gravitational field of the Galaxy on apparent celestial positions of extragalactic sources was theoretically investigated, and statistical characteristics of this process for some realistic models of our Galaxy were obtained. It was shown that the jitter, caused by stars or other massive object moving closely to the line of sight, increases with the observational interval and reached some maximal value which depends on the sky direction. In particular, on the scale of 10 years, the deviation of the apparent source position from the true one can reach several tens of μas in the direction towards the Galactic Center, decreasing down to 1-3 μas at high galactic latitudes. It is important to note, that in contrast to the random walk of the particle, the observed fluctuations of the source position occur relative to some “true” position. In general, the functional properties of this effect

is determined by its autocorrelation function and power spectrum (see Paper I for details).

As it follows from calculations, the jitter effect is quite small. Nevertheless, advances of observational techniques prompt us to pose a question about its observability. It can be important for at least two reasons. Firstly, the detection of such a jitter poses a fundamental limit on the astrometric accuracy. Secondly, a comparison of jitter parameters with theoretical predictions will help us in the future to validate the model of the Galaxy used for computations.

A number of environmental factors – such as mismodelling of path delay in the neutral atmosphere, mismodelled crustal deformations caused by the mass loading (Petrov & Boy 2004), imperfections of the Earth rotation model (Petrov 2007) – affects the accuracy of the absolute radio astrometry. Although some authors claimed that the accuracy of the VLBI absolute astrometry can reach 0.05 mas (Fey et al. 2015), we adhere a more conservative estimate of the accuracy floor at the level of 0.15 mas. If not a single object but a pair of objects is observed, the environmental factors are diluted roughly proportional to the objects angular separation, and thus the accuracy of the differential astrometry can reach dozens of μas per single epoch (Reid & Honma 2014; Martí-Vidal et al. 2010). It should be noted that the differential astrometry cannot provide positions of observed objects, only a difference in positions.

This work is a second one in the cycle of papers dedicated to the study of the gravitational noise of the Galaxy and its influence on the positional accuracy of extragalactic sources. Here, we consider a possibility to detect this jitter effect using high-precision radio interferometric observations. The problem to be solved is formulated in Section 2. In Section 3, we estimate the uncertainties of the expected effect due to an imperfect knowledge of parameters of the Galaxy models, the mass and velocity distribution functions of deflecting bodies, as well as due to an algorithm of the numerical calculations. The other possible effects that can cause the observed offset between the two sources are briefly discussed in Section 4. Section 5 presents the main steps in the experiment simulation. Obtained results and some observational issues are discussed in Section 6.

2. THE PROBLEM FORMULATION

Let’s consider two groups of bright extragalactic sources – “target” and “control” samples. Each sample includes N closely spaced pairs of sources. Sources of the target sample are located at $|b| \leq 1.5^\circ$ and $|l| \leq 20^\circ$ (where l and b are galactic longitude and latitude, correspondingly), i.e. within the Galactic plane close to the Galactic Center, where the expected value of the standard deviation of the jitter effect (hereafter “jitter std”) is maximal. Sources of the control sample are located at high galactic latitudes, $|b| \geq 30^\circ$, where the jitter std is predicted to be significantly lower. Measur-

ing arc lengths between pairs for these two samples and performing a statistical analysis of the data obtained, we expect to detect a systematic increase of the standard deviation in arc lengths of pairs in the “target” group with respect to the “control” one on a time scale of several years.

For illustration purposes, we show one particular realisation of simulated samples of extragalactic sources on the map of the conditional standard deviation of the angular jitter for the observational interval of 10 years (Fig. 1). From this figure it is easy to see that in the absence of any additional noise, besides the jitter effect, the standard deviations (and dispersions) for these samples should differ by several times. Thus, in this “ideal” case, it is possible to establish the difference between two samples of sources at the high significance level. However, the jitter effect will be observed against a background of various noises, both instrumental and astrophysical, that can prevent its detection in real data.

Moreover, before simulating an experiment, we need to assess uncertainties associated with the theoretical calculations of the jitter std provided in Paper I. The latter are based on the present-day mass function (PDMF) of stars, the velocity and spatial distribution of these stars (the Galaxy model) as well as some simplifying assumptions. It is obvious that uncertainties of parameters of models and functions will affect the amplitude of the effect. Thus, our primary task is to calculate the whole budget of possible errors arising due to these uncertainties, as well as due to the algorithms of numerical calculations. Below, we consider all these issues which affect detectability of the jitter effect.

3. UNCERTAINTIES OF THE THEORETICAL MODELLING

According to Paper I, the spatial, velocity and PDFM distribution functions are independent, therefore the uncertainty for the jitter std can be estimated as summation in quadrature of uncertainties of each of the distribution functions. Below we consider them separately.

3.1. Galactic models

Our non-accurate knowledge of the structure of the Galaxy is the first and the main problem which leads to the modelling uncertainties. In Paper I, all calculations were carried out for two models of the density distribution of the matter in the Galaxy: 1) the “classical” Bahcall-Soneira model (Bahcall & Soneira 1980; Bahcall 1986) and 2) the more realistic model of the Galaxy of Dehnen & Binney (1998, (their model 2)). For convenience, let’s call the latter one as the ‘basic’ model. It is necessary to note that this model is only one out of four models which were obtained by these authors from the analysis of the same observational data. Therefore, in order to assess how much the choice of the Galaxy model affects our estimates of the jitter std across the sky, we performed its calculations for three other models

from Dehnen & Binney (1998, models 1, 3, and 4), and for the Galaxy model from McMillan (2017), which was constructed using latest observational data.

Using the same technique as in Paper I, we constructed a set of maps of the jitter std for different models of the Galaxy. A comparison of these maps shows that, depending on the used model, variations of the jitter std are about several percent at high galactic latitudes, increasing to 20 – 25% in the central part of the Galaxy and low latitudes. Such an increase in uncertainty is connected with difficulties of the parametrization of the central part of the disk and the bulge components. For the following estimations, we used 25% as a conservative value of the uncertainty of the jitter std due to our non-accurate knowledge of the exact structure of the Galaxy.

3.2. Present-day mass functions

It is well known that the mass function of Galactic stars can not be determined directly from observations. Observable quantities, e.g., the luminosity function or the surface brightness, are transformed into the mass function through the mass-age-luminosity relation. Thus the mass function is obtained within the framework of a given theory of a stellar evolution.

In our calculations, we used universally recognized present-day mass functions for the disc, halo and bulge stars from papers of Chabrier & Mera (1997); Chabrier (2003). Expressions for PDMFs of different galactic components include two or three parameters, which are determined within given uncertainties. Obviously, the scatter in the PDMFs parameters affects the results obtained in Paper I. We varied the parameters of PDMFs randomly within the intervals of their uncertainties and estimated the resulting uncertainty on the jitter std to be 9-15%, depending on the sky direction and contribution of different galactic components. For our following calculations, we use 15% as a conservative value of the uncertainty on the jitter std due to our non-accurate knowledge of the mass functions.

3.3. Stellar velocity distribution

A velocity distribution of stars, used in Paper I, depends on two parameters: the escape velocity from the Galaxy and the dispersion of the stellar velocities, which are different for different galactic components. Variations of the escape velocity within 10% of its value 500 km s^{-1} do not have any noticeable impact on the jitter std. Variations of the stellar velocity dispersions within their uncertainties, reported by Bland-Hawthorn & Gerhard (2016) for different galactic components, lead to the variations in the jitter std which are below 5%.

Thus the uncertainty due to our non-accurate knowledge of the stellar velocity distribution can be conservatively estimated as 5%.

Finally, uncertainties of the conditional standard deviations or the autocorrelation functions can be as large as 20%, depending on the choice of the minimal impact parameter of a deflecting body in respect to the observable extragalactic source (see Paper I for details).

Summarizing all above, an overall ‘theoretical’ uncertainty on the jitter std, arising due to different types of the modelling uncertainties, can be conservatively estimated as 35%.

4. OTHER NOISES

Let’s consider other possible effects that affect measurements of the arc length between two sources. They are as follows: 1) thermal noise; 2) the contribution of path delay in the ionosphere; 3) the contribution of path delay in the neutral atmosphere. Atmospheric errors grow approximately linearly with the source separation, therefore, the shorter the separation, the better. Martí-Vidal et al. (2010) provided realistic estimates of differential astrometry errors as a function of source separation. At the 2° separation, the accuracy of $30 \mu\text{as}$ can be achieved with the interferometer baselines of $\sim 2000\text{--}3000 \text{ km}$ (Honma, private communication). Reid & Honma (2014) noted that random errors of differential astrometry for the 1° source separation can even reach $\sim 10 \mu\text{as}$ for the interferometer baseline of $\sim 8000 \text{ km}$, although systematic errors are usually higher.

One has to take into consideration several other factors. First, the structure for many AGNs is changing with time, that is related to their flaring activity (see, e.g., Lister et al. 2019, and references therein). During a flare, a component is ejected from the core regions, travels with the relativistic speed, then fades out and disappears. Presence of an extended jet, if left unaccounted for, typically contributes to estimates of source positions at the level of $30\text{--}100 \mu\text{as}$. However, if a jet has a compact component, in extreme cases its contribution to the source position may surpass 1 mas according to recent results of Petrov & Kovalev (2017). Changes in the source structure due to the evolution of jet components, if unaccounted for, result in the change of source position estimates. This effect can be modelled using source maps, however the question on the residual errors of the source contribution accounted that way remains open.

Another phenomenon is a core-shift. The core position is shifted along the jet due to self-absorption, and this shift is frequency dependent. The effect was predicted by Blandford & Königl (1979) theoretically and then confirmed from observations (see, e.g., Kovalev et al. 2008; Sokolovsky et al. 2011, and references therein). A typical value of the core-shift at 8 GHz is about $200 \mu\text{as}$. Recently Plavin et al. (2019) has demonstrated a variability of the core-shift related to the flaring activity. The core-shift is reduced at high frequencies, although as Abellán et al. (2018) has shown, it is still at the level of $100 \mu\text{as}$ at 15 GHz. Thus, multi-frequency observations are needed to evaluate the core-shift and its evolution.

Another non-stability of the source position and broadening of the image can be caused by scattering in the interstellar medium (Pushkarev & Kovalev 2015; Lazio et al. 2008). The broadening is common at low galactic latitudes, and in the extreme cases a source cannot be detected at long baselines at 1–8 GHz due to broadening. Since the astrometric accuracy of VLBI is reciprocal to the baseline length, a loss of long baselines reduces astrometric accuracy. Moreover, clouds of the interstellar medium can change the broadening, and such variations associated with extreme scattering events may happen at scales of months (Pushkarev et al. 2013; Cimò et al. 2002; Fiedler et al. 1987, 1994). The broadening is reciprocal to frequency squared, and observations at high frequencies, 22 GHz and higher, substantially mitigate this effect.

The impact of these effects can be minimized, if one observes close pairs of sources (separated by no more than $1\text{--}2^\circ$) at high frequencies, i.e. at 22 GHz or higher, and performs simultaneous observations at several frequencies (at least, at two) to evaluate the core-shift and estimate the remaining frequency-dependent ionospheric contribution.

5. EXPERIMENT SIMULATION

In this section, we carry out an experiment simulation guided by the above recommendations on the observation strategy.

We start with generating two samples of distant sources. The target sample, consisting of N source pairs, is created at random in the central sky region with coordinates $|b| \leq 1.5^\circ$ and $|l| \leq 20^\circ$. The separation in the pair varies from 1° to 2° . A lower limit of separation is set due to absence of spatial correlation of the jitter effect. As discussed in previous Section, the accuracy of the differential VLBI astrometry starts to degrade noticeably when the separation exceeds 2° due to short-term variations in path delay through the atmosphere. The initially specified arc lengths in the pair of sources is considered as the “true” one¹.

The choice of the longitude/latitude for the control sources is determined by the minimal value of the effect. In general, control sample sources should have the latitude greater than 30° (see Fig. 1). Here, the control sample is created in the sky region $-70^\circ \leq l \leq -20^\circ$ and $30^\circ \leq b \leq 60^\circ$ in the same way as the target sample.

As soon as two samples are generated, at the next stage we need to simulate “observational” data, taking into account the studied jitter effect as well as an influence of different types of noise. The experiment simulation includes three steps: 1) first, we generate an array of “measured” arc lengths in each pair in the absence of any noise other than the jitter effect; 2) then, we

synthesize three types of noise - white, flicker and red - that represent different types of observational and instrumental noises; 3) finally, we produce and analyze a noisy signal.

Now we consider all these steps in details.

5.1. Signal generation

The main purpose of this subsection is to simulate the jitter effect with the predicted statistical parameters in the absence of any other noise.

Let’s assume that we observe N closely spaced pairs of sources of the target and control samples K times during T years. After T years, we expect to have N time sequences consisting of K measured arc lengths between sources of the i -th pair $l_i(t_j)$, where $j = 1, \dots, K$, in a given (target or control) sample. To simulate the noise-free observation of the jitter effect, we generate arrays of “measured” arc lengths $l_i(t_j)$ under the following assumptions:

1. the jitter std of sources in each i -th pair, α_{i1} and α_{i2} , are independent (since the minimum separation between sources in a pair is chosen to avoid a spatial correlation);
2. values of α_{i1}^2 and α_{i2}^2 for a given time interval between observations are calculated according to the predicted autocorrelation function of the jitter effect from Paper I;
3. the generated arc lengths l_i between sources in the i -th pair are drawn from the Gaussian distribution with an average value equal to the “true” arc length l_i^{true} (since the mathematical expectation of the jitter vector is zero), and with the std $\alpha_{tot}(t)$, which depends on time;
4. in its turn, $\alpha_{tot}(t)$ is also distributed over the Gaussian with the mean of $\mu = \sqrt{\alpha_{i1}^2(t) + \alpha_{i2}^2(t)}$ and the width of $\varepsilon \simeq 0.35\mu$, where 35% is the ‘theoretical’ uncertainty on the jitter std discussed in Section 3.

As soon as we have the array of “measured” arc lengths $l_i(t_j)$ for the i -th pair of sources, we can calculate the average arc length for a given pair as $\langle l_i \rangle = \frac{1}{K} \sum_{j=1}^K l_i(t_j)$ and subtract this value from each “measured” arc length. Thus, for each i -th pair of sources we obtain a sequence of arcs $\Delta l_i(t_1), \dots, \Delta l_i(t_K)$, where $\Delta l_i(t_j) = l_i(t_j) - \langle l_i \rangle$. This sequence is called a signal for the i -th pair. A similar procedure is performed for all the N pairs from the target sample. As a result, we obtained the matrix $[K \times N]$ of arcs $\Delta l_i(t_j)$, which is one of the possible realizations of our measurements for the target sample. This matrix was used to calculate

¹ Of course, in real observations this parameter is unknown. Here it is needed only as a starting point for further modelling.

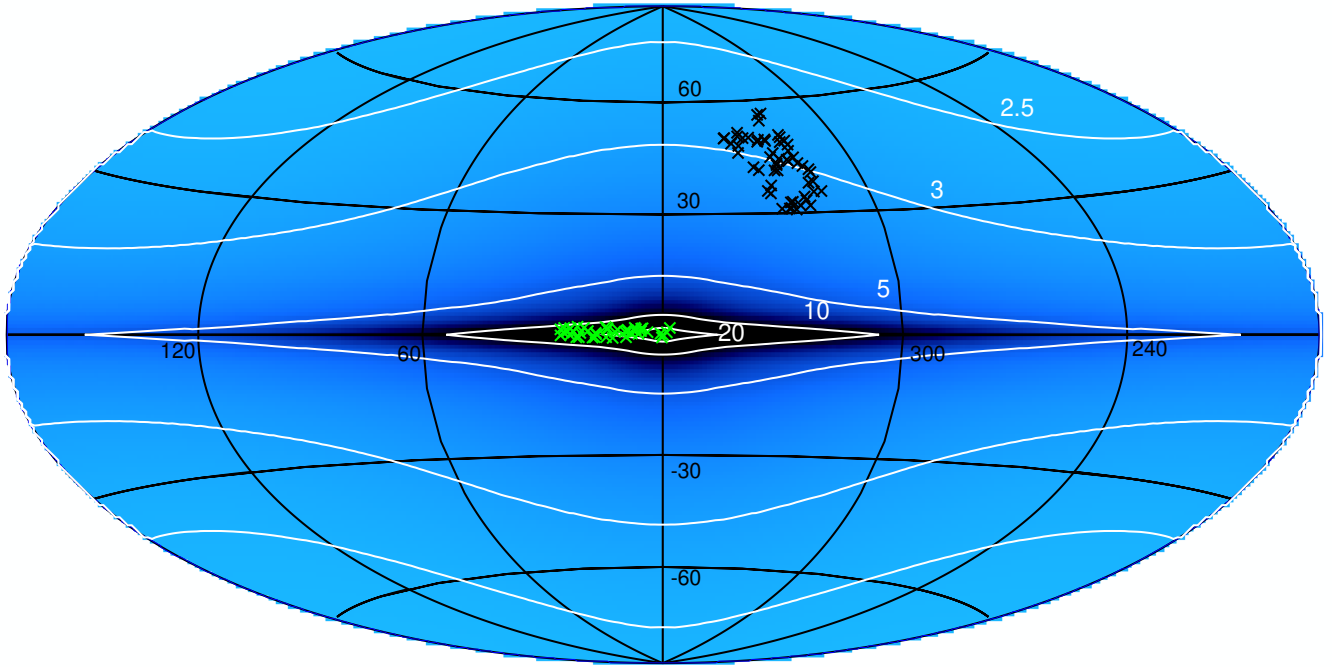


Figure 1. Map of the conditional standard deviation of the angular jitter (in μas) for the observational interval of 10 years. White lines show contours of the jitter angle $\alpha = 20, 10, 5$ and $3 \mu\text{as}$. Positions of the target (in green) and control (in black) sources are marked as crosses.

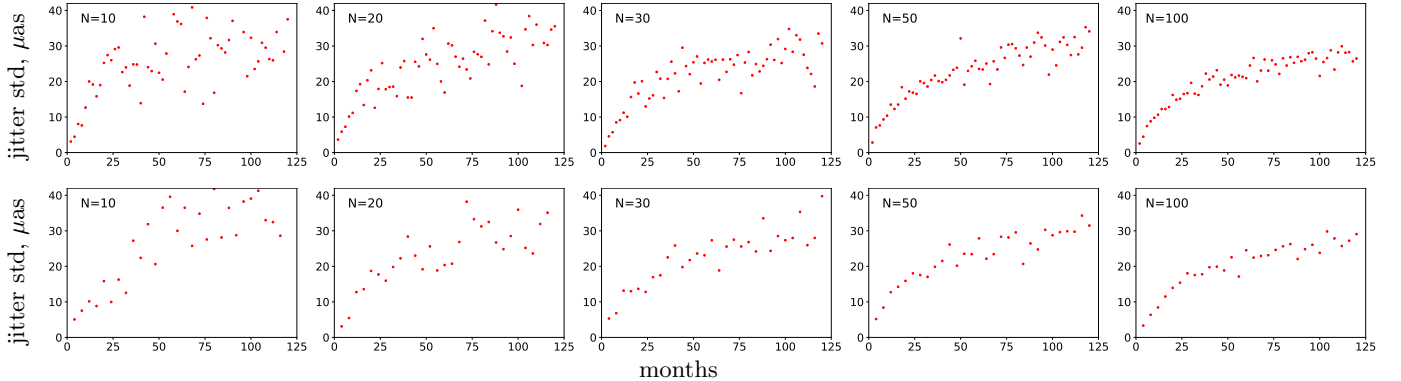


Figure 2. The jitter std as a function of time (in months) for different number of source pairs ($N=10, 20, 30, 50$ and 100) from the target sample. Only one random realization is shown. In the upper row, the sampling interval between observation is equal to 2 months, in the lower row, the interval is equal to 4 months.

the standard deviation for this random realization in the appropriate way².

² Throughout the paper, we calculate the standard deviation as $\sigma = \sqrt{\frac{\sum_{k=1}^K (x_k - \langle x \rangle)^2}{K-1}}$, where $\{x_1, x_2, \dots, x_K\}$ are the observed values, $\langle x \rangle$ is the mean value, and K is the number of observations in the sample. The variance is denoted as σ^2 .

It is obvious that for each of the possible realizations the calculated standard deviation of the arc lengths will be different. To define the mean value of the jitter std and its scatter, we performed 100 such realizations. We tested that increasing the number of realizations above 100 doesn't lead to any change in derived quantities at $1 \mu\text{as}$ level. So, the spread of the average value of the obtained jitter std determines the range of expected val-

ues of that can be obtained in the experiment with no extra-noises.

The described above algorithm is carried out for the pairs of the control sample as well. As a result, we obtain 100 matrices $[K \times N]$ of arc lengths $\Delta l_i(t_j)$ and calculate the average value of the jitter std and its spread for both target and control samples.

Now it is important to estimate how many pairs of sources, what duration and the duty cycle of observations are needed for the adequate statistical analysis. The scatter of the average value of the jitter std obviously depends on the number of pairs of sources as $1/\sqrt{N}$. Even in the idealized noise-free experiment, for 10 pairs of sources, an expected growth with time of the standard deviations of measured arc lengths could be buried under random fluctuations (see Fig. 2), while for $N = 30$, the trend with time can be clearly recognized. There is no doubt that the larger the number of source pairs, the more accurate the statistics. Nevertheless, for observational reasons, it is necessary to determine a sufficient number of pairs for the purposes of our experiment (Fig. 2). So hereafter, we concentrate on the target and the control samples, consisting of $N = 30$ pairs of sources each. Figure 3 represents the mean value of the jitter std with no extra-noises and its scatter for 30 pairs of target (red lines) and control (grey lines) sources as a function of time for different sampling intervals between observations: 2, 4 and 6 months. For the target sample, the mean value of std increases with time and reaches $\simeq (25 \pm 4) \mu\text{as}$ after 5 years of observations and $\simeq (30 \pm 5) \mu\text{as}$ after 10 years. For the control sample, the mean value of std varies slightly with time and approximately equals to $(3 \pm 1) \mu\text{as}$ after 10 years of observations. The slope of the signal power spectrum equals to $\simeq -2$ as derived in Paper I.

Note, that the sampling interval does not noticeably affect the jitter curve (top panel of Figure 3), since the smooth curves were obtained by averaging over a large number of realizations of the experiment. However, in a real experiment, only a single sequence of observations (as opposed to 100 realizations in our calculations) is available. In such a case, increasing the frequency of observations obviously leads to more accurate estimates of mean pairwise arc lengths. Figure 3 (lower panels) illustrates how for one random realization the cumulative moving average arc length between sources in a pair converges with time. Measurements for each of 30 pairs of sources are marked with grey dots. Red lines show the mean value of $\Delta = \langle l \rangle - l^{true}$, where $\langle l \rangle$ is the cumulative moving average arc lengths at the time instance t , and the uncertainty (one standard deviation) on this mean.

5.2. Noisy signal

In the previous section, we have simulated an ideal experiment with no extra-noises except for the noise from the jitter effect, which is considered to be the useful sig-

nal here. Now we consider the more realistic situation when this useful signal is ‘‘spoiled’’ by the noise.

Different effects that cause the non-stability of the source position and proposed a strategy to minimise them were discussed in Section 4. Not all the arising noises/effects are well understood and can be completely removed from observational data. Here, we assume that the jitter is spoiled with some kind of noise left after the data cleaning process. Since the jitter effect is different in nature from other astrophysical noises (such as a flaring activity of AGN, core shift, scattering in the interstellar medium, etc), as well as from instrumental noises, we do not expect any correlation between the useful signal (the jitter effect) and the noise. Thus, we assume that the noise is additive. In the following analysis we consider three types of noise: white noise, flicker noise (the spectrum with $1/f$) and red noise (the spectrum with $1/f^2$) as the most common in the analysis of time series in Astronomy and Meteorology Press (1978); Scargle (1981); Vaughan (2013).

The white noise time sequence for each pair of sources is drawn from a Gaussian distribution with a zero mean and a given variance σ_n^2 . A colored noise (with a power law power spectrum) is generated using the algorithm described in Timmer & Koenig (1995). The average value of the noise amplitude in each time sequence is set to zero, the mean variance of noise time sequences is σ_n^2 . As an example, one realization of different types of the noise with some given value of σ_n^2 is shown in Fig. 4. The upper panel of the figure shows the dependence of the noise amplitude on time, where the white noise is shown in blue, the flicker noise is in red and the red noise is in green. The bottom panel of the figure shows the power spectrum, where the blue dashed line is a constant (the white noise), red corresponds to the spectrum with $1/f$ (the flicker-noise), green corresponds to the spectrum with $1/f^2$ (the red noise).

As in the case of the signal generation, 100 realizations of the noise amplitude matrix for three types of noise with a given power spectrum and variance were obtained for simulating the ‘‘spoiled’’ signal.

To obtain a noisy signal, the noise amplitude matrix is added to the signal amplitude matrix for each realization. As a result, we have 100 matrices $[K \times N]$ of ‘‘noisy’’ arc lengths $\Delta l_i(t_j)$ for both target and control samples, where $N=30$. These matrices were analyzed in the same way as for the matrices of pure signal (see Section 5.1).

We assume that the signal is spoiled by only one type of noise, either white or colored, with $\sigma_n = 10 \mu\text{as}$ and $\sigma_n = 30 \mu\text{as}$. As mentioned in Section 4 these values roughly correspond to the level of differential astrometry errors for different interferometer baselines (Reid & Honma 2014). Note that all types of the noise give the similar result as long as: (i) calculations are performed for the fixed number of source pairs, and (ii) the noise variance remains the same for different col-

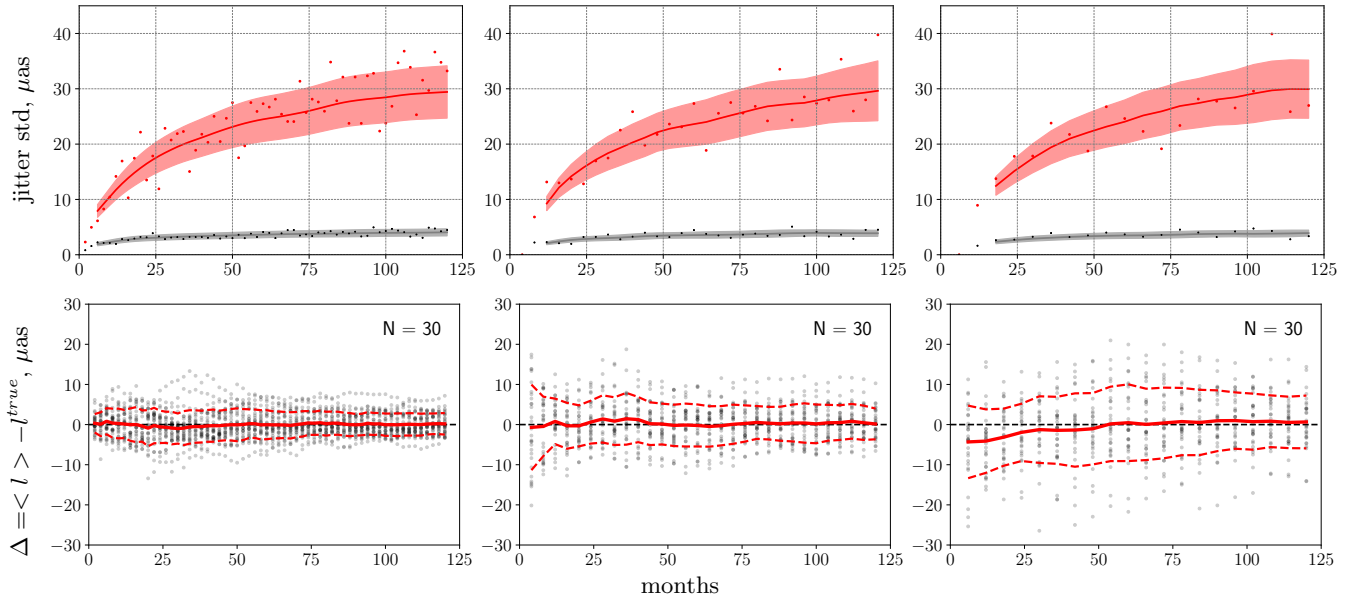


Figure 3. *The upper panels:* the jitter std as a function of time. From left to right: observations are made each 2, 4, and 6 months, respectively. Red and grey thick lines show the mean value of the jitter std for 100 realizations of target and control samples, respectively. The uncertainties are shown by the red and grey shaded areas, for the target and control sources. Red and grey dots represent one random realization for the target and control sources, respectively. *The lower panels:* the cumulative moving average arc lengths between 2 sources converge with time to its true value. Grey dots show measurements for each of 30 pairs of sources. Red lines show the mean value of $\Delta = \langle l \rangle - l^{\text{true}}$ and the uncertainty (by dashed lines) on this mean (see text for details).

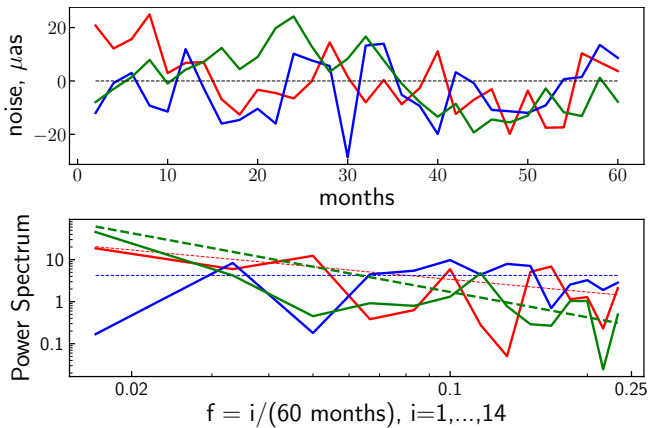


Figure 4. Illustration of different types of noise considered in the paper. The upper panel shows the dependence of the noise amplitude in μas versus time. White noise is shown in blue, the flicker noise is in red, the red noise is in green. The bottom panel shows the power spectrum. The blue dashed line is a constant (white noise), red is $1/f$ (the flicker-noise), green is $1/f^2$ (the red noise), where $f = i/(60 \text{ months})$, $i = 1, \dots, 14$ is a (discrete) Fourier transform frequency.

ors of the noise. Taking this into account we show in Fig. 5 the std and its spread assuming that the signal is spoiled by the white noise only. We conduct averaging over 100 realizations of a noisy signal, as in the analysis

of the signal with no extra-noises. Thick lines show how the mean std of measured arc lengths between sources in pairs increases with time. Shaded dark areas represent the uncertainty on the mean (i.e. one standard deviation), shaded light areas represent three standard deviations. Statistical properties were calculated for a sample of 100 realizations. Red and grey dots are the std of the noisy signals for one random realization of the target and control samples, respectively. According to the Fisher criterion, one can distinguish between the target and control samples at least at the 3σ -level, if light red shaded area lies above the horizontal dashed line.

It can be seen that for our choice of σ_n , the standard deviation and its spread for the control sample are entirely determined by the noise. Figure 5 also shows that for the target sample the scatter of the standard deviation increases with the duration of experiment which is owing to the presence of the “jitter” effect, in contrast to the control sample, where the time variation is practically constant with time. As follows from our calculations, on the scale of ~ 2 years, it would be possible to detect a systematic increase in the std of measured arc lengths of pairs of target sources compared to the control ones at the 3σ -level (according to the Fisher criterion) if the accuracy of differential astrometric observations is $10 \mu\text{as}$.

6. SUMMARY AND DISCUSSION

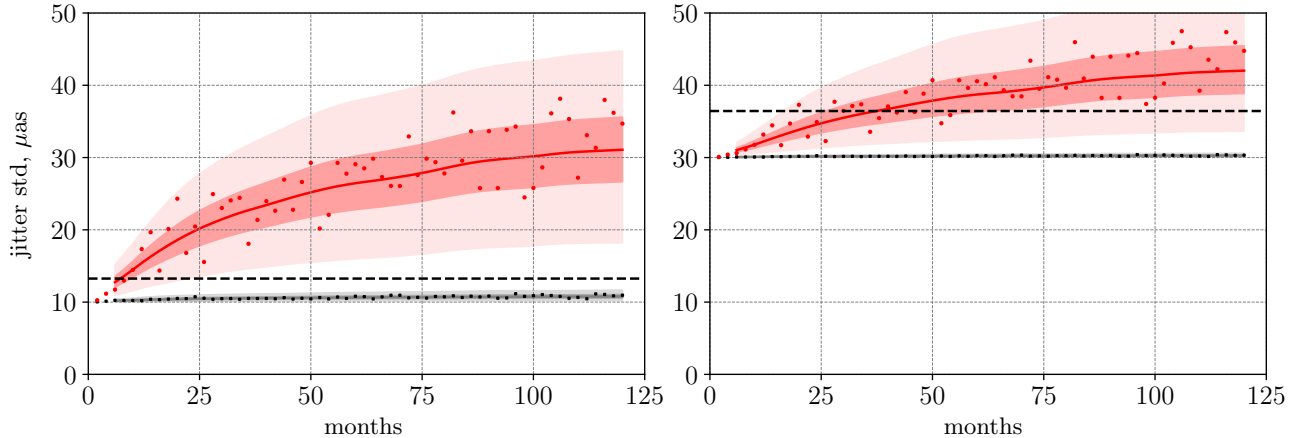


Figure 5. Prospects for detecting the jitter effect in ‘noisy’ observations. The thick lines show how the mean std of measured arc lengths between sources in pairs increases with time. Shaded dark areas represent the uncertainty on this mean (i.e. one standard deviation), shaded light areas represent 3 standard deviations. Observations are made each 2 months. Left and right panels show the curves for the jitter signal spoiled by an additive noise with the mean variance of $\sqrt{\sigma_n^2} = 10 \mu\text{as}$ and $30 \mu\text{as}$, correspondingly. The statistical properties were calculated for a sample of 100 realizations. One random realization is shown with dots. Red and grey color are used for the target and the control sample, correspondingly. According to the Fisher criterion, the target and control samples can be distinguished at the 3σ -level, if the light red shaded area lies above the dashed thick horizontal line.

Motions of stars and compact objects in our Galaxy cause local fluctuations of its gravitational field which lead to jittering of apparent celestial positions of distant sources. In Paper I, it was found that the jitter amplitude depends on a direction in the sky and can reach several tens of microarcsecond.

In this paper, we considered the possibility of detecting the jitter effect on the basis of the theoretical predictions of its value and the current accuracy of the differential astrometry. We simulated long-term measurements of the arc lengths of the closely spaced source pairs divided into two groups: “target” and “control”. Target sources lie in the direction to the central part of the Galaxy, where the expected jitter effect is maximal, while control sources are located at high galactic latitudes, where the predicted jitter amplitude is minimal. Different types of physical and instrumental noises were taken into account in the form of the additive extra-noise (white, red, and flicker) with a constant dispersion in time.

It was shown that on the scale of ~ 2 years, it is possible to detect a systematic increase in the std of measured arc lengths of pairs of target sources compared to the control ones at the 3σ -level (according to the Fisher criterion) if the noise dispersion σ_n is $10 \mu\text{as}$. If σ_n is $30 \mu\text{as}$, then the target and control samples will differ only at the 2σ -level on the scale of 10 years, that can be considered as a possible hint for the jitter effect. These values of σ_n roughly correspond to the level of differential astrometry errors for different interferometer’s baseline (Reid & Honma 2014). Note the accuracy

of $\sim 20 \mu\text{as}$ is necessary to achieve the 3σ -level on 10 years interval.

We make a conclusion that measurement of extra jitter is achievable with the current technology of radioastronomical observations, although a great case should be taken for assessment of the contribution of systematic errors and characterization of their power spectrum. The distribution function of the observed arc lengths has a potential to differ the Galactic models. As it was shown in Section 3.1, the difference in the jitter values can reach 25% for the explored models, presumably in central parts of the Galaxy. Thus, the accuracy of astrometric measurements at the level of few μas is required to resolve this task.

We also discussed other possible effects that can also affect the arc length measurements between two sources. To make the detection of the astrometric jitter in the Galaxy possible, one should minimize them. It can be achieved by (1) observing close pairs of sources (within $1\text{--}2^\circ$ to each other), (2) observing at high frequencies (22 GHz and higher), and (3) observing at least at two frequencies simultaneously to evaluate the core-shift and solve for frequency-dependent remaining ionospheric contribution. Zhao et al. (2018) have shown how this can be done in practice. Systems like VERA and KVN that offer simultaneous 22/43 GHz capabilities and just recently have demonstrated $30 \mu\text{as}$ astrometric accuracy, as well as proposed ngVLA, that will cover the frequency range from 1.2 to 112 GHz (Selina et al. 2018) seem the most promising in these aspects.

REFERENCES

- Abellán, F. J., Martí-Vidal, I., Marcaide, J. M., & Guirado, J. C. 2018, *A&A*, 614, A74, doi: [10.1051/0004-6361/201731869](https://doi.org/10.1051/0004-6361/201731869)
- Bahcall, J. N. 1986, *ARA&A*, 24, 577, doi: [10.1146/annurev.aa.24.090186.003045](https://doi.org/10.1146/annurev.aa.24.090186.003045)
- Bahcall, J. N., & Soneira, R. M. 1980, *ApJS*, 44, 73, doi: [10.1086/190685](https://doi.org/10.1086/190685)
- Beasley, A. J., Gordon, D., Peck, A. B., et al. 2002, *ApJS*, 141, 13, doi: [10.1086/339806](https://doi.org/10.1086/339806)
- Bland-Hawthorn, J., & Gerhard, O. 2016, *ARA&A*, 54, 529, doi: [10.1146/annurev-astro-081915-023441](https://doi.org/10.1146/annurev-astro-081915-023441)
- Blandford, R. D., & Königl, A. 1979, *ApJ*, 232, 34, doi: [10.1086/157262](https://doi.org/10.1086/157262)
- Chabrier, G. 2003, *PASP*, 115, 763, doi: [10.1086/376392](https://doi.org/10.1086/376392)
- Chabrier, G., & Mera, D. 1997, *A&A*, 328, 83. <https://arxiv.org/abs/astro-ph/9705065>
- Cimò, G., Beckert, T., Krichbaum, T. P., et al. 2002, *PASA*, 19, 10, doi: [10.1071/AS01097](https://doi.org/10.1071/AS01097)
- Dehnen, W., & Binney, J. 1998, *MNRAS*, 294, 429, doi: [10.1046/j.1365-8711.1998.01282.x](https://doi.org/10.1046/j.1365-8711.1998.01282.x)
- Dominik, M., & Sahu, K. C. 2000, *ApJ*, 534, 213, doi: [10.1086/308716](https://doi.org/10.1086/308716)
- Fey, A. L., Gordon, D., Jacobs, C. S., et al. 2015, *AJ*, 150, 58, doi: [10.1088/0004-6256/150/2/58](https://doi.org/10.1088/0004-6256/150/2/58)
- Fiedler, R., Dennison, B., Johnston, K. J., Waltman, E. B., & Simon, R. S. 1994, *ApJ*, 430, 581, doi: [10.1086/174432](https://doi.org/10.1086/174432)
- Fiedler, R. L., Dennison, B., Johnston, K. J., & Hewish, A. 1987, *Nature*, 326, 675, doi: [10.1038/326675a0](https://doi.org/10.1038/326675a0)
- Kovalev, Y. Y., Lobanov, A. P., Pushkarev, A. B., & Zensus, J. A. 2008, *A&A*, 483, 759, doi: [10.1051/0004-6361/20078679](https://doi.org/10.1051/0004-6361/20078679)
- Larchenkova, T. I., Lutovinov, A. A., & Lyskova, N. S. 2017, *ApJ*, 835, 51, doi: [10.3847/1538-4357/835/1/51](https://doi.org/10.3847/1538-4357/835/1/51)
- Lazio, T. J. W., Ojha, R., Fey, A. L., et al. 2008, *ApJ*, 672, 115, doi: [10.1086/520572](https://doi.org/10.1086/520572)
- Lindgren, L., Hernandez, J., Bombrun, A., et al. 2018, *A&A*, A14. <https://arxiv.org/abs/1804.09366>
- Lister, M. L., Homan, D. C., Hovatta, T., et al. 2019, *ApJ*, 874, 43, doi: [10.3847/1538-4357/ab08ee](https://doi.org/10.3847/1538-4357/ab08ee)
- Martí-Vidal, I., Ros, E., Pérez-Torres, M. A., et al. 2010, *A&A*, 515, A53, doi: [10.1051/0004-6361/201014203](https://doi.org/10.1051/0004-6361/201014203)
- McMillan, P. J. 2017, *MNRAS*, 465, 76, doi: [10.1093/mnras/stw2759](https://doi.org/10.1093/mnras/stw2759)
- Petrov, L. 2007, *A&A*, 467, 359, doi: [10.1051/0004-6361:20065091](https://doi.org/10.1051/0004-6361:20065091)
- Petrov, L., & Boy, J.-P. 2004, *Journal of Geophysical Research (Solid Earth)*, 109, B03405, doi: [10.1029/2003JB002500](https://doi.org/10.1029/2003JB002500)
- Petrov, L., & Kovalev, Y. Y. 2017, *MNRAS*, 471, 3775, doi: [10.1093/mnras/stx1747](https://doi.org/10.1093/mnras/stx1747)
- Plavin, A. V., Kovalev, Y. Y., Pushkarev, A. B., & Lobanov, A. P. 2019, *MNRAS*, 485, 1822, doi: [10.1093/mnras/stz504](https://doi.org/10.1093/mnras/stz504)
- Press, W. H. 1978, *Comments on Astrophysics*, 7, 103
- Pushkarev, A. B., & Kovalev, Y. Y. 2015, *MNRAS*, 452, 4274, doi: [10.1093/mnras/stv1539](https://doi.org/10.1093/mnras/stv1539)
- Pushkarev, A. B., Kovalev, Y. Y., Lister, M. L., et al. 2013, *A&A*, 555, A80, doi: [10.1051/0004-6361/201321484](https://doi.org/10.1051/0004-6361/201321484)
- Reid, M. J., & Honma, M. 2014, *ARA&A*, 52, 339, doi: [10.1146/annurev-astro-081913-040006](https://doi.org/10.1146/annurev-astro-081913-040006)
- Scargle, J. D. 1981, *ApJS*, 45, 1, doi: [10.1086/190706](https://doi.org/10.1086/190706)
- Selina, R. J., Murphy, E. J., McKinnon, M., et al. 2018, in *Astronomical Society of the Pacific Conference Series*, Vol. 517, *Science with a Next Generation Very Large Array*, ed. E. Murphy, 15
- Sokolovsky, K. V., Kovalev, Y. Y., Pushkarev, A. B., & Lobanov, A. P. 2011, *A&A*, 532, A38, doi: [10.1051/0004-6361/201016072](https://doi.org/10.1051/0004-6361/201016072)
- Timmer, J., & Koenig, M. 1995, *A&A*, 300, 707
- Vaughan, S. 2013, *arXiv e-prints*, arXiv:1309.6435. <https://arxiv.org/abs/1309.6435>
- Yano, T. 2012, *ApJ*, 757, 189, doi: [10.1088/0004-637X/757/2/189](https://doi.org/10.1088/0004-637X/757/2/189)
- Zhao, G.-Y., Algaba, J. C., Lee, S. S., et al. 2018, *AJ*, 155, 26, doi: [10.3847/1538-3881/aa99e0](https://doi.org/10.3847/1538-3881/aa99e0)
- Zhdanov, V. I., & Zhdanova, V. V. 1995, *A&A*, 299, 321